Zika Virus–Associated Micrencephaly

A Thorough Description of Neuropathologic Findings in the Fetal Central Nervous System

Peter Štrafela, MD; Alenka Vizjak, PhD; Jerica Mraz, BSc; Jernej Mlakar, MD; Jože Pižem, MD, PhD; Nataša Tul, MD, PhD; Tatjana Avšič Županc, PhD; Mara Popović, MD, PhD

• ***Context.***—**The 2015 outbreak of Zika virus in Brazil resulted in a 20-times increased prevalence of congenital microcephaly in stillborns and neonates and was instrumental in raising the suspicion of a causal association between Zika virus and microcephaly.**

Objective.—**To provide a comprehensive description of the neuropathologic features of congenital Zika virus infection.**

Design.—**Autopsy evaluation of the brain from a fetus of 32 weeks and 6 days of gestation, with a prenatal diagnosis of microcephaly associated with polymerase chain reaction–confirmed, fetal, Zika virus infection.**

Results.—**Multiple severe pathology findings were present. These included lissencephaly, except for the occipital lobes, where some pachygyria was observed. Also present was reduction and thinning of white matter, ventriculomegaly of the lateral ventricles, and coalescent calcifications in the cortical-subcortical white matter border associated with glioneuronal outbursting into the subarachnoid space above and heterotopias below. There were small, scattered calcifications in the basal ganglia, with fewer in the white matter and germinal matrix, and none in the cerebellum and brainstem. The cerebellum and pontine base were atrophic because of Wallerian degeneration or maldevelopment of descending tracts and pontocerebellar connections.**

Conclusion.—**Our findings are in agreement with neuroimaging of Zika virus–associated fetal and infant micrencephalic brains and, to some extent, with neuroimaging of other intrauterine infections causing microcephaly.**

(*Arch Pathol Lab Med*. 2017;141:73–81; doi: 10.5858/arpa.2016-0341-SA)

Microcephaly ("small head") is usually a consequence of fetal brain maldevelopment resulting in micrencephaly ("small brain"). The development of the fetal brain can be affected by various pathologic events causing micrencephaly, such as genetic, metabolic (maternal phenylketonuria or poorly controlled diabetes), toxic (maternal alcohol abuse, radiation, or hydantoin), ischemic, and infectious etiologies.[1–4] It is well recognized that some microorganisms are especially prone to affect the developing fetal brain, and some have been put together under the acronym TORCH (*Toxoplasma gondii*, others, varicella-zoster virus, rubella, cytomegalovirus, and herpes simplex virus).[5] In addition to micrencephaly, frequent findings in the brains of fetuses affected by TORCH agents include ventriculomegaly, encephalomalacic pseudocysts, atrophic corpus callosum, polymicrogyria, cerebellar hypoplasia, and calcifications, which can usually be detected by neuroimaging.[6] Some cases with fetal, intracranial, bandlike calcifications, similar to those produced by TORCH agents but without confirmed intrauterine viral infection, have been described under the term pseudo-TORCH.[7,8]

The most-frequent microorganisms affecting the fetal brain and causing microcephaly, usually accompanied by calcifications, are cytomegalovirus and *Toxoplasma gondii*.[6] An outbreak of microcephaly in Brazil, causally associated with the Zika virus epidemic since May 2015, has resulted in this emerging viral infection becoming the leading causative agent of microcephaly in South and Central America[9,10] and a serious threat to pregnant women from other countries who have visited that region.[11,12]

Fetal brain pathology associated with intrauterine Zika virus infection has usually been diagnosed by neuroimaging techniques used during pregnancy and after childbirth.[13–15]

Zika virus belongs to the group of Flaviviruses, some of which can be vertically transmitted, usually with no intrauterine fetal brain damage.[16,17] An exception is the report of intrauterine West Nile virus transmission occurring at 30th weeks' gestation in which the female infant, delivered at 38 weeks, had ocular and brain damage discovered by magnetic resonance imaging (MRI) but no microcephaly.[18]

We describe the case of a European woman infected by Zika virus while in Brazil. Vertical transmission resulted in fetal brain damage with micrencephaly and calcifications.[11]

Accepted for publication September 1, 2016.

Published as an Early Online Release October 11, 2016.

From the Department of Pathology, University Clinical Centre, Maribor, Slovenia (Dr Štrafela); the Institutes of Pathology (Drs Vizjak, Mlakar, Pižem, and Popović and Mrs Mraz) and Microbiology and Immunology (Dr Županc), Faculty of Medicine, University of Ljubljana, Ljubljana, Slovenia; and the Department of Perinatology, Division of Gynecology and Obstetrics, University Medical Centre, Ljubljana, Slovenia (Dr Tul).

The authors have no relevant financial interest in the products or companies described in this article.

Reprints: Mara Popović, MD, PhD, Institute of Pathology, Faculty of Medicine, University of Ljubljana, Korytkova 2, 1000 Ljubljana, Slovenia (email: mara.popovic@mf.uni-lj.si).

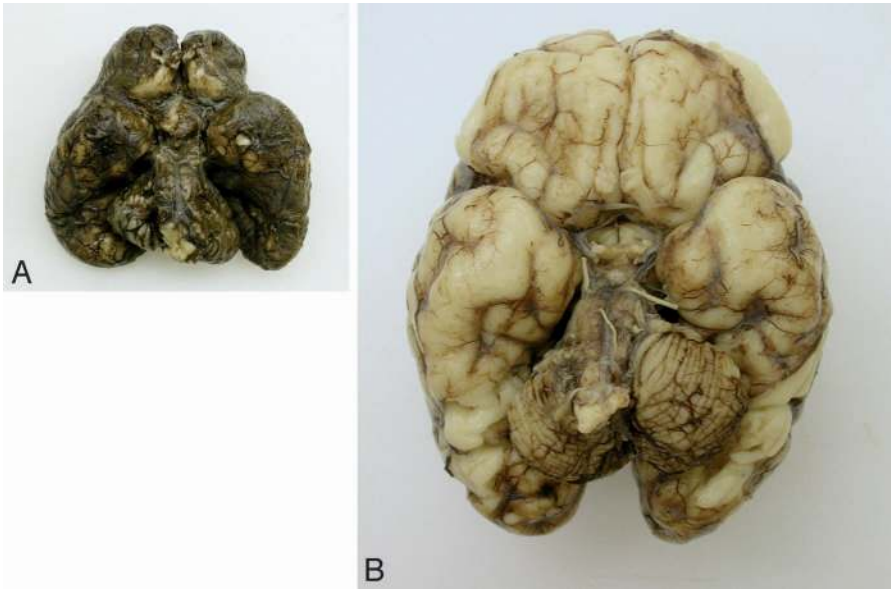

Figure 1. *Gross presentation of the cerebrum, cerebellum, and brainstem of the Zika-infected brain (A) and age-matched control (B).*

In this report, the detailed gross and microscopic pathology abnormalities in the central nervous system of the fetus after autopsy are discussed.

CLINICAL HISTORY

A pregnant woman in the 13th week of gestation became symptomatic in May 2015, with fever, myalgia, arthralgia, generalized maculopapular rush, retroocular pain, and conjunctivitis. She had lived in the northeastern region of Brazil since 2013, which had recently become an endemic area for the Zika virus. Because she was suspected of having Zika virus infection, additional testing was performed. Obstetrical ultrasounds performed in the 14th and 22nd weeks of gestation did not show fetal abnormalities. When she returned to Europe, ultrasonography performed in the 29th week of gestation showed fetal brain abnormalities, including microcephaly, ventriculomegaly, widespread calcifications, and cerebellar atrophy. Additionally, an MRI performed in the 31st week of gestation showed encephalomalacic pseudocysts and cortical maldevelopment, which was interpreted as polymicrogyria. With maternal written informed consent, termination of pregnancy was performed at the 32nd week and sixth day of gestation. Three days later, a male stillborn baby was delivered, and an autopsy was performed. Except for microcephaly, all other gross findings were unremarkable. Fresh tissue from the placenta, brain, and other organs were taken for viral molecular genetic analysis, and Zika virus was found only in the brain tissue. All other possible neurotropic microorganisms (TORCH infections, dengue virus, and Chikungunya virus) were excluded as possible causal agents of the fetal brain damage.[11]

NEUROPATHOLOGY

Macroscopic Features

After removal from the skull, the fetal brain was fixed for 3 weeks in 27% formalin containing NaCl and ZnSO4. The whole brain was small, weighing 84 g, which is 3-fold lighter than the average fetal brain in the 33rd week of gestation (reference range, 240 g). The cerebellum and brainstem weighed 13 g, whereas in the case of healthy, age-matched controls the weight of these structures is 17 g, indicating that the subtentorial part of the brain was also atrophic (Figure 1, A and B). The leptomeninges were dark due to hyperemia, and subarachnoid hemorrhage was induced by the feticide procedure. Gyration was almost absent compared with healthy, age-matched controls (Figure 2, A through F). Irregular, white calcifications at the cortical–white matter border were visible, mostly in the frontal and to a much lesser extent in the parieto-occipital regions but not in the temporal lobes (Figures 2, B and C, and 3). In addition, the lateral ventricles were enlarged more prominently in the parieto-occipital region, and a large encephalomalacic cyst was present in the right occipital lobe (Figures 2, C, and 3). In spite of strong fixation lasting 3 weeks, the corpus callosum split apart, and temporal lobes partially fell apart during brain sectioning; the right hippocampus could not be recognized and sampled (Figure 3). Gyri were completely absent on the coronal sections in the frontotemporal regions, and the Sylvian fissure was wide open. Some wide gyri were present in the parieto-occipital regions, compatible with pachygyria (Figure 3). Subcortical nuclei and the left hippocampus were well preserved, and the third ventricle was narrow (Figure 3).[11]

Microscopic Features

Microscopic examination revealed that the left hippocampus and entorhinal cortex were well organized. The neocortex was unevenly disorganized, showing the most-disturbed organization in the frontal lobes. In that location, large, focal, coalescent calcifications were present at the cortical–white matter border, associated with heterotopias below them, and glioneuronal outbursts into the subarach-

→

Figure 2. *Gross pathology of Zika-infected brain weighing 84 g (A, B, and C) and age-matched control weighing 240 g (D, E, and F). A, Artificial subarachnoid hemorrhage due to termination of pregnancy. Tissue taken for molecular genetic analysis (asterisks). B, Agyria, calcifications (arrows), and ventriculomegaly in frontal lobes. C, Pachygyria, ventriculomegaly, pseudocysts (asterisks), and calcifications (arrow) in occipital lobes. D, Appropriate gyration for 33rd week of gestational age. E and F, Frontal and occipital lobes with appropriate gyration and lateral ventricles, respectively.*

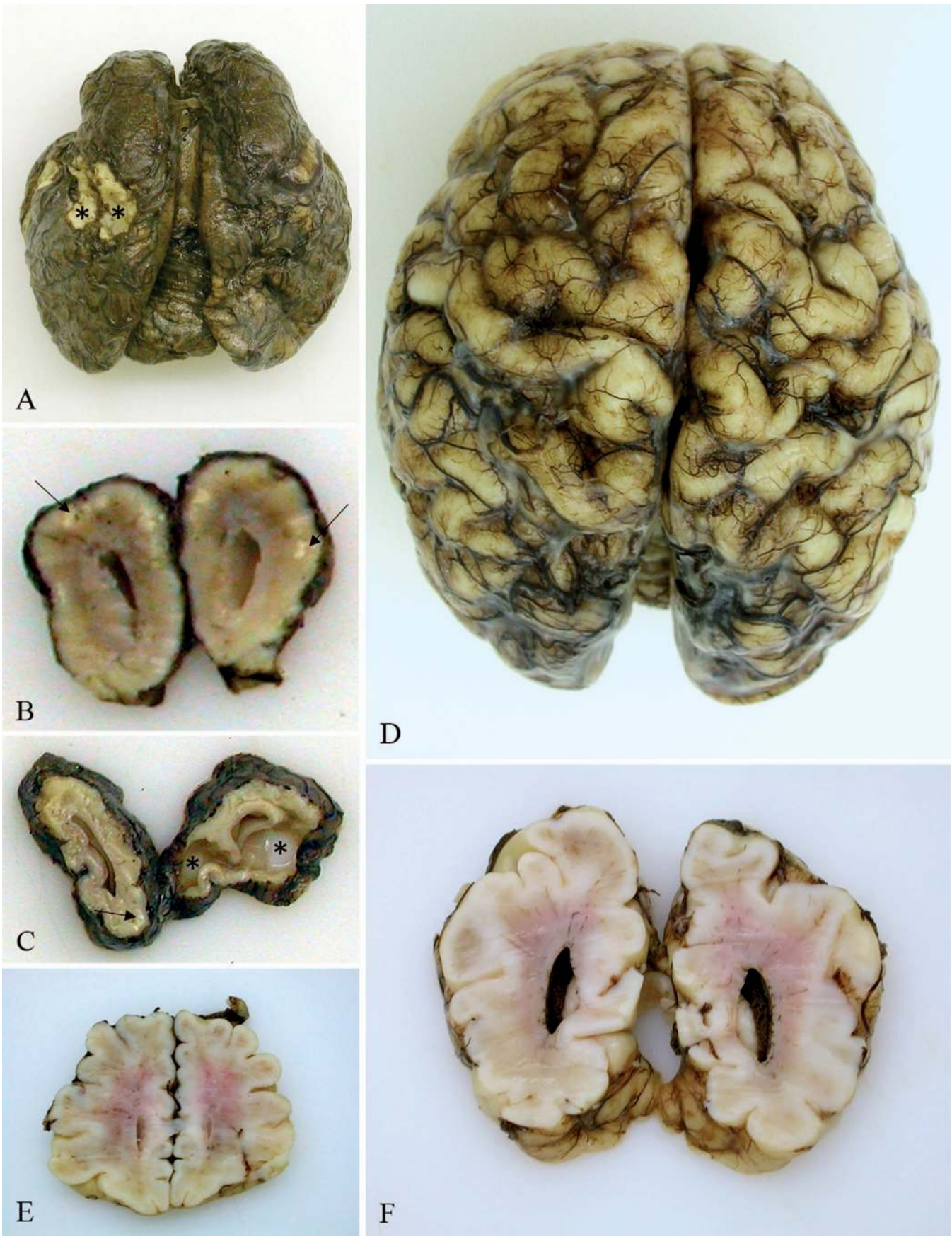

Figure 3. *Coronal sections of the fetal brain from frontal (upper-left corner) to occipital (lower-right corner).*

noid space above them, which can be termed *heterotopias*, as well (Figure 4, A through D).

Preservation of the cortical cellular morphology was poor, probably due to several factors, such as retained (arrested) differentiation of the migrating neurons, the feticide procedure, which is harmful for brain tissue per se, followed by 3 days of intrauterine autolysis. It was almost impossible to differentiate developing cortical neurons from glial cells. Three of the neuronal antibodies (NF protein, clone 2F10, DakoCytomation, Glostrup, Denmark; nonphosphorylated neurofilament SMI32, Covance, Princeton, New Jersey; MAP2, clone AP20, Merck Millipore, Darmstadt, Germany) used did not label the neuronal cell bodies (Table). Neurofilament immunohistochemistry using 2 monoclonal antibodies (neuronal antibodies and SMI32) showed very thin fascicles of the axons in the white matter and internal capsule and some uneven neuronal processes in the subarachnoidal glioneuronal outbursts (Figure 4, D). No microscopic features of polymicrogyria were observed. Neuronal marker NeuN (clone A60, Merck Millipore) labeled the nuclei of the very few developed cortical neurons and a considerable number of neurons in the subcortical nuclei and brainstem. Microscopic examination of the HLA-DR and CD68 (DakoCytomation, Glostrup, Denmark) immunostains did not show any significant differences in the distribution and cellularity of macrophages or in activated microglial cells throughout the telencephalon and were almost absent inside the encephalomalacic pseudocyst of the right occipital lobe.

Subcortical nuclei, basal ganglia, and thalami were well organized and preserved and contained mature neurons.

The germinal matrix was moderately cellular for gestational age, as compared with the age-matched control. Some small foci of siderophages and very few microcalcifications were present (Figure 5, D).

White matter of the telencephalon was considerably reduced, especially in the parieto-occipital region. Myelination was not recognized at all using Kluver-Barrera–specific staining.

Calcifications

There were macroscopically visible, coalescent calcifications composed of numerous, small calcifications of various shapes at the cortical–white matter border (Figure 5, A). In addition, there were scattered, small microcalcifications ($\leq$50 μm diameter) in the cortex as well as in the subcortical nuclei (Figure 5, B and C). Frequently, the microcalcifications in the subcortical nuclei were located in a perivascular distribution, but no vessel-wall calcifications were observed (Figure 5, C). Very rarely, the microcalcifications were present in the white matter and in the periventricular

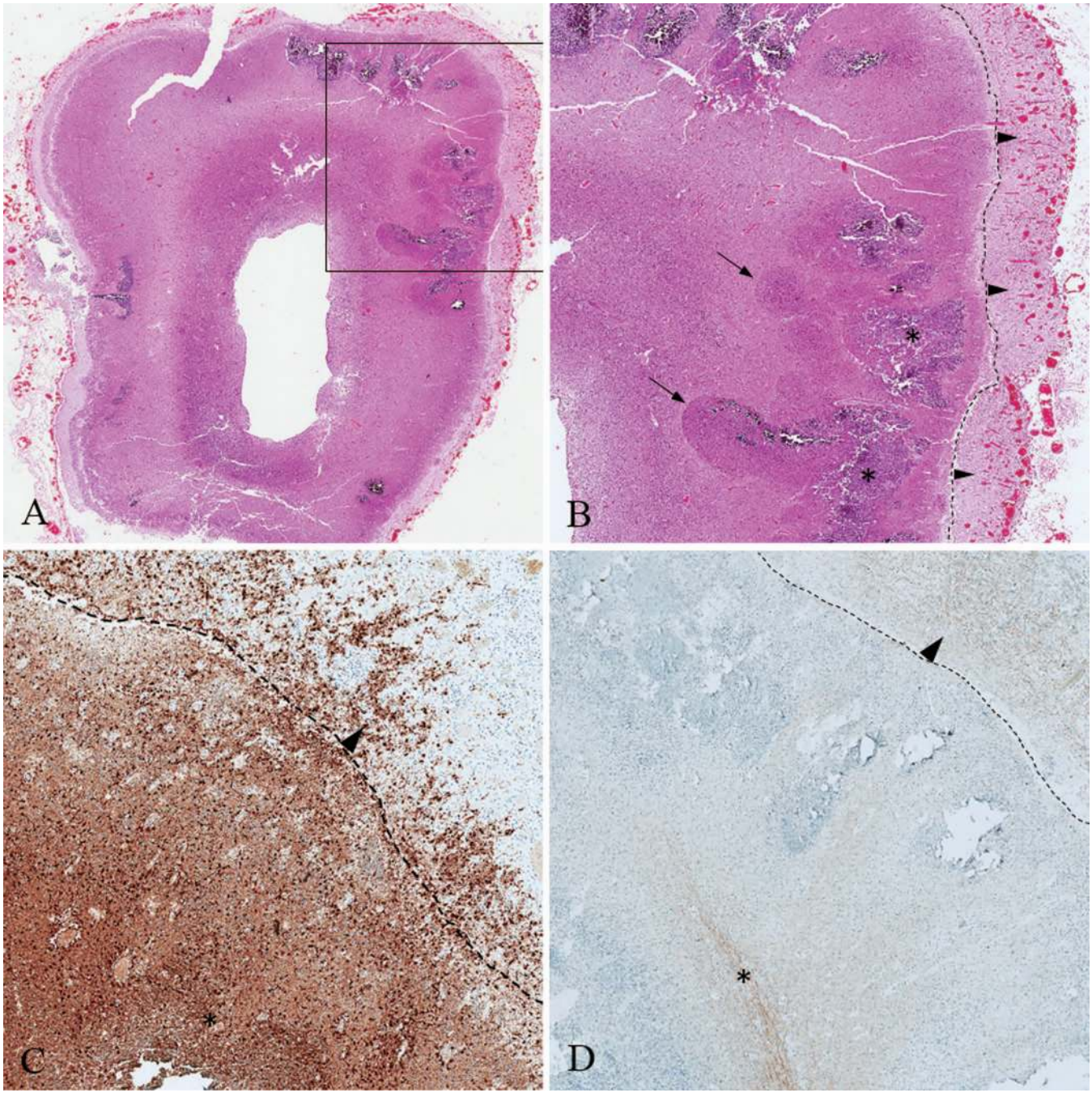

Figure 4. *Cortical pathology. A, The entire left frontal hemisphere. B, Magnified image of the rectangle in A; glioneuronal outbursting through the pial surface, labeled with a dashed line and arrowheads, calcifications (asterisk), and heterotopias (arrows). C and D, Glial and neuronal components of the outbursts (dashed line with arrowhead), respectively, with a bundle of axons in D (asterisk) (hematoxylin-eosin, original magnifications, ×8 [A] and ×200 [B]; GFAP [glial fibrillary acidic protein; clone 6F2, DakoCytomation, Glostrup, Denmark], original magnification ×300 [C]; nonphosphorylated neurofilament [SMI32, Covance, Princeton, New Jersey] original magnification, ×300 [D]).*

germinal matrix (Figure 5, D). No microcalcifications were present in the cerebellum and brainstem.

Cerebellar and Brainstem Atrophy

The cerebellum and brainstem were well organized but both, especially the pontine base, were much smaller than that of the age-matched control (Figure 6, A and B, respectively). This was probably due to Wallerian degeneration and/or to arrested development of the corticospinal and corticobulbar tracts, as well as pontocerebellar connections, which were well demonstrated by neurofilament immunostaining (Figure 6, C and D). Maldevelopment of the corticospinal and other descending tracts was also obvious in the spinal cord.[11]

Inflammation

Inflammation was not a prominent feature in the brain.[11] Only a few foci of mild perivascular cuffing were present in the white matter of the telencephalon. The inflammatory cells composing these cuffs were mostly T lymphocytes

The Antibodies Used in the Zika Virus Study				
Antibody	**Clone**	**Antigen Retrieval**	**Dilution**	**Producer**
GFAP	6F2	—	1:100	DakoCytomation, Glostrup, Denmark
NF protein	2F11	EDTA pH 9	1:100	DakoCytomation, Glostrup, Denmark
Nonphospho-NF protein	SMI32	EDTA pH 9	1:200	Covance, Princeton, New Jersey USA
NeuN	A60	EDTA pH 9	1:1000	Merck Millipore, Darmstadt, Germany
MAP2	AP20	EDTA pH 9	1:8000	Merck Millipore, Darmstadt, Germany
CD68	PGM1	EDTA pH 9	1:50	DakoCytomation, Glostrup, Denmark
HLA-DR	TAL1B5	EDTA pH 9	1:10	DakoCytomation, Glostrup, Denmark
CD3	LN10	EDTA pH 9	1:15	Novocastra, Newcastle Upon Tyne, England
CD8	C8/144B	EDTA pH 9	1:50	DakoCytomation, Glostrup, Denmark
CD20	L26	EDTA pH 9	1:400	DakoCytomation, Glostrup, Denmark
Maternal IgG antibodies		Citrate buffer pH 6	1:10	
Anti-Flavivirus group antigen	4G2	Citrate buffer pH 6	1:10	Absolute Antibody, Oxford, England

Abbreviations: GFAP, glial fibrillary acidic protein; HLA-DR, human leukocyte antigen DR; IgG, immunoglobulin G; MAP2, myelin-associated protein; NF, neurofilament.

(stained with CD3, Novocastra, Newcastle Upon Tyne, England), together with some macrophages (CD68 stain). No perivascular cuffing was present in the brainstem or cerebellum. Scattered T lymphocytes (CD3 stain) were present throughout the brain tissue, including the subarachnoid glioneuronal outbursts but were rare in the cerebellum. Activated microglia (HLA-DR) and macrophages (HLA-DR and CD68) were numerous in all regions of the telencephalon and moderately frequent in the pontocerebellar peduncles and pontine base, but only rare HLA-DR$^+$ cells were present in the white matter of the cerebellum (figure not shown).

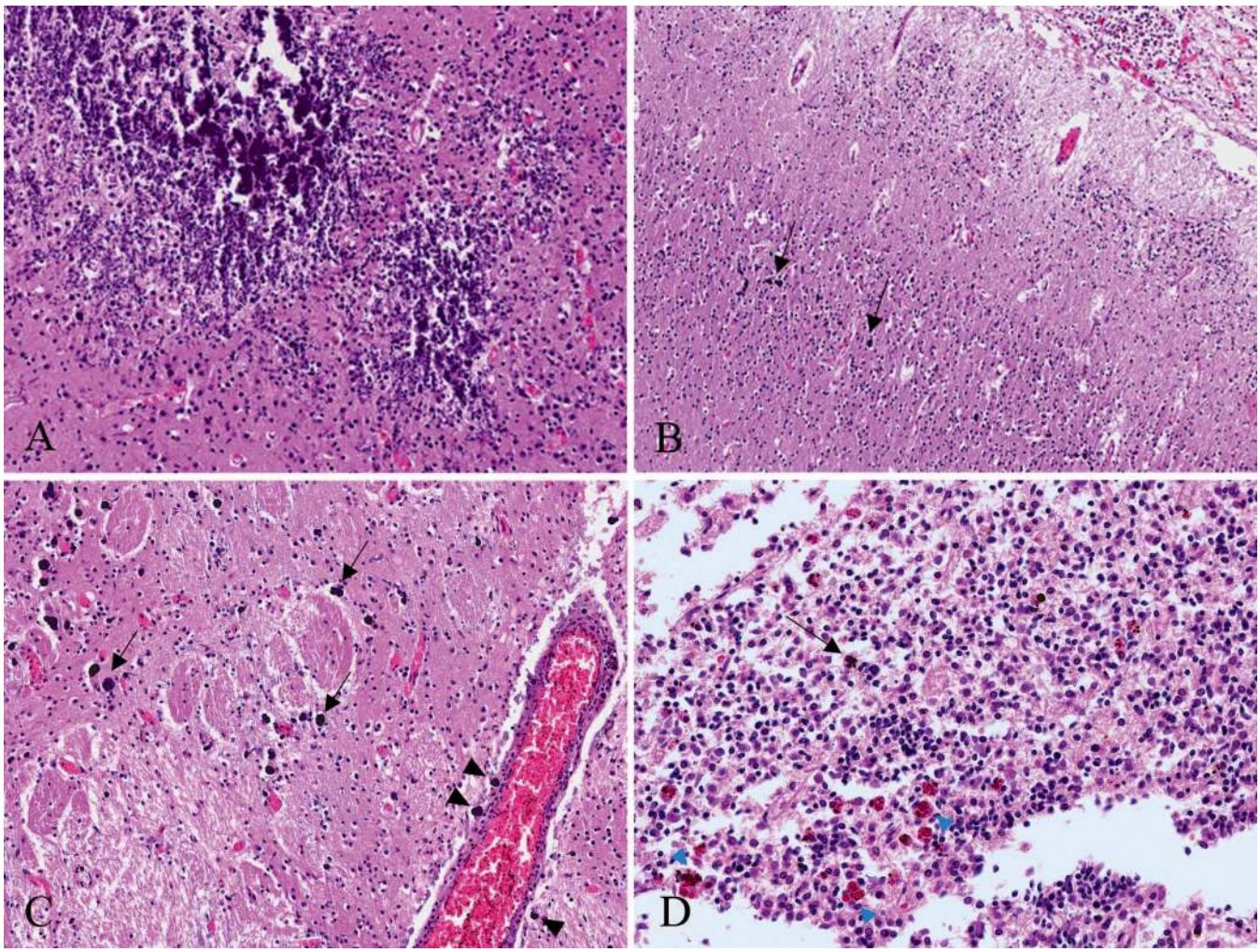

Figure 5. *Calcifications. A, Macroscopically visible calcifications at the cortical–white matter border are composed of numerous, variously shaped microcalcifications. B, Additional scattered microcalcifications are present inside the cortex (arrows). C, Microcalcifications in the striatum (arrows) were seen frequently in perivascular locations (arrowheads). D, Very few microcalcifications in the germinal matrix (black arrow) were accompanied by focal siderophages (blue arrowheads) (hematoxylin-eosin, original magnification ×400 [A through D]).*

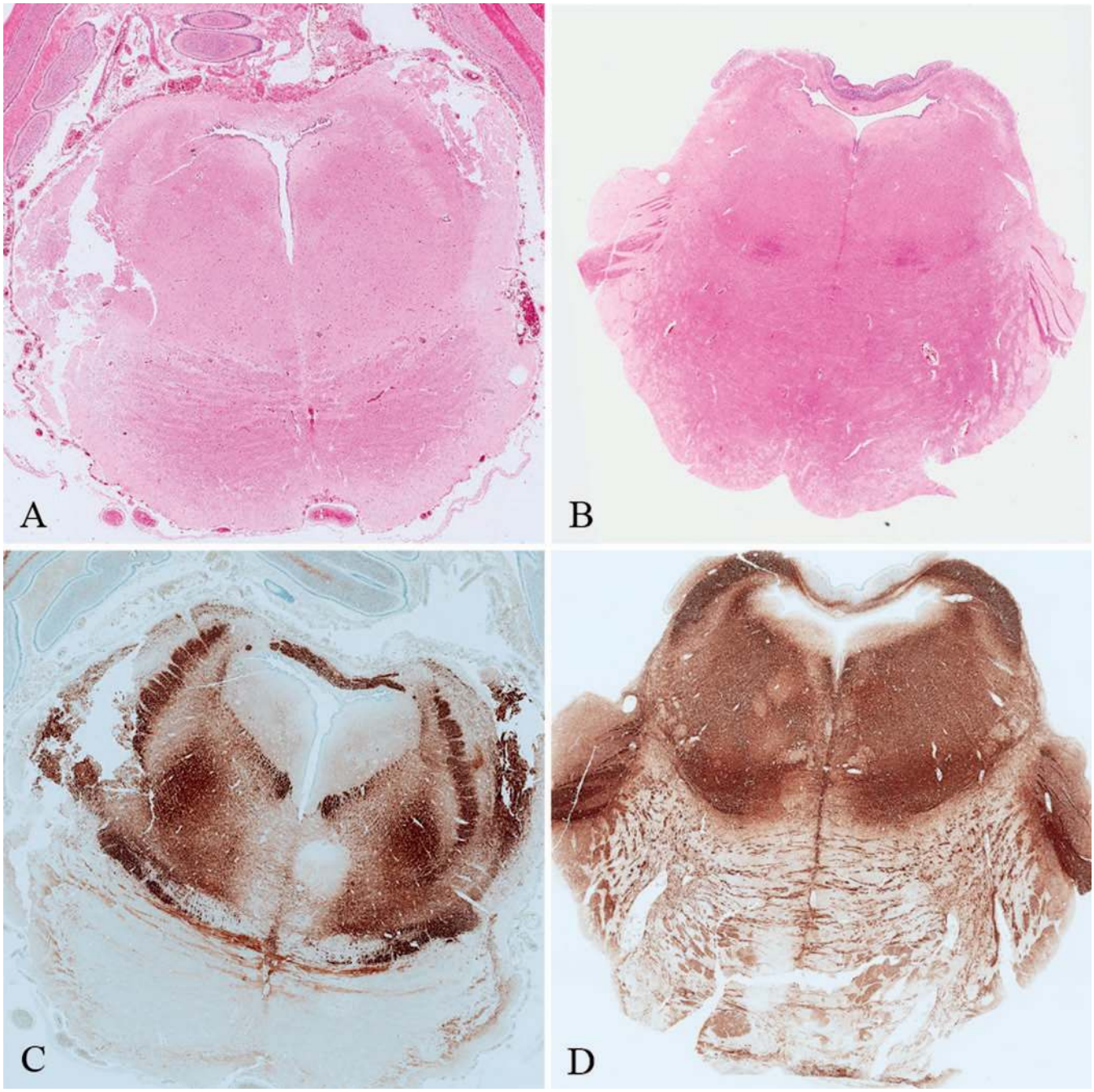

Figure 6. *The pons of Zika-infected brain (A and C), compared with an age-matched control (B and D). A and B, Pontine base is smaller in the Zika-infected brain (A). C and D, Descending tracts and most of the pontocerebellar connections are not displayed in Zika-infected brain (C) (hematoxylin-eosin, original magnification ×8 [A and B]; nonphosphorylated neurofilament [SMI32, Covance, Princeton, New Jersey], original magnification ×8 [C and D]).*

Zika Virus Detection by Indirect Immunofluorescence and Electron Microscopy

Slides with paraffin sections of the frontal lobe of the fetal brain and the unaffected age-matched control were stained with recombinant monoclonal antibody to Flavivirus group antigen (D1-4G2-4-15 [4G2]) from Absolute Antibody (Oxford, England) and maternal sera containing immunoglobulin G antibodies against Zika virus, using the indirect immunofluorescence technique to determine viral localization. The 4G2 anti-Flavivirus antibody did not result in any positive immunofluorescence staining, whereas maternal sera showed that the virus was located preferentially in the cortical plate (Figure 7, A). Rare positive signals were found in the leptomeningeal outbursts and in the germinal matrix, but there was not any signal identified in the white matter. After omission of the primary antibody (maternal serum), no signal was present in the cortical section adjacent to that area (Figure 7, A and B).

Small samples of the fetal cortex were taken from the formalin-fixed brain tissue for electron microscopy. A group of viral particles consistent with Zika virus were found in

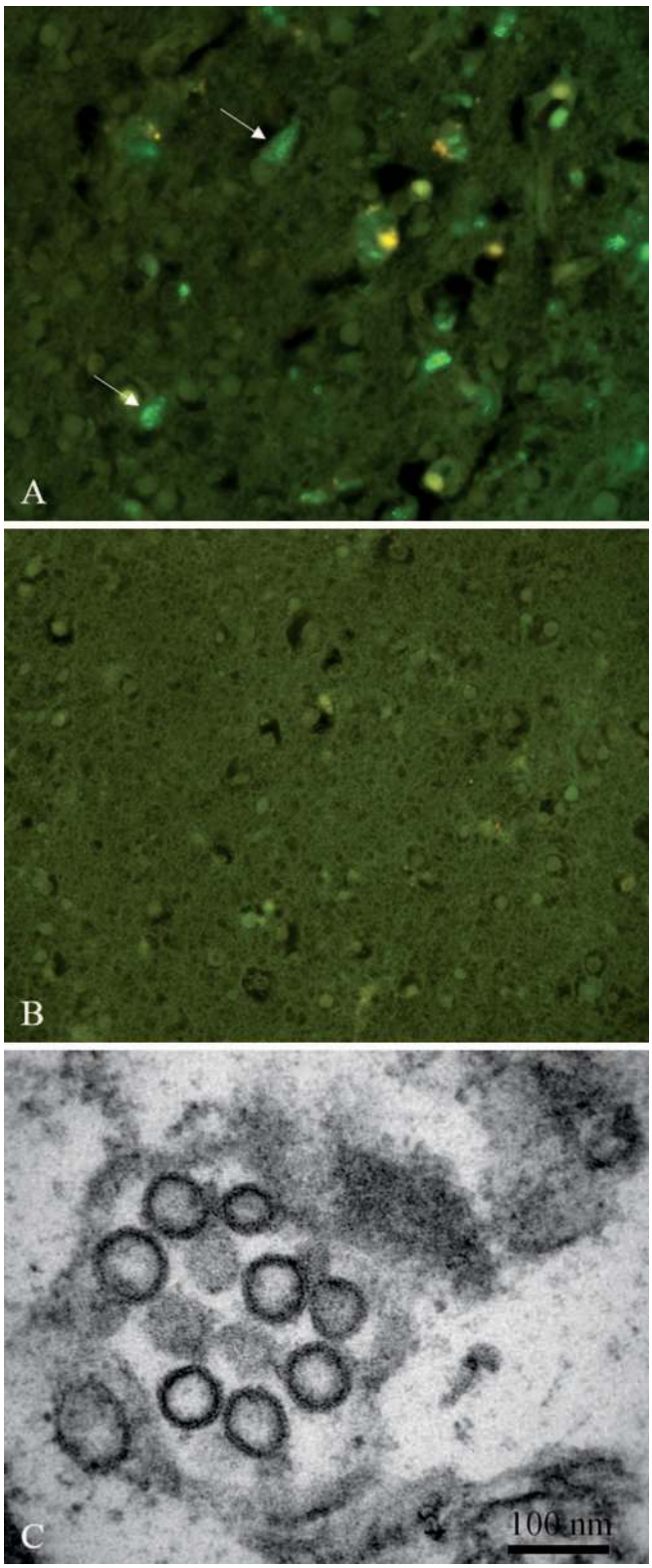

Figure 7. *Zika virus in fetal brain tissue. A, Zika virus was detected mostly in the cortical cells (arrows). B, Zika-infected brain cortex with an omitted maternal primary antibody as negative control. C, Ultrastructure of the viral particles consistent with the Zika viruses (indirect immunofluorescence [IIF] with maternal immunoglobulin G antibodies [A]; IIF with omission of maternal immunoglobulin G antibodies [B]; electron microscopy [C]).*

autolyzed cells without preserved cell membranes or recognizable intracellular structures, so that the precise cell type affected by the virus could not be determined (Figure 7, C).

DISCUSSION

Although the increased occurrence of microcephaly associated with the current Zika virus pandemic in Brazil and other countries of South and Central America has been observed since 2015,[19,20] few descriptions of the neuropathologic findings from the brains of infected fetuses have been reported.[11,12,21] Most fetal brain abnormalities have been diagnosed by prenatal neuroimaging, using obstetrical ultrasonography and, in fewer cases, by MRI techniques.[12,13,22] The neuroimaging presentation of brain pathology associated with prenatal Zika virus infection correlates well with our postmortem findings of micrencephaly and cortical malformations, white matter reduction, ventriculomegaly, encephalomalacic pseudocysts, calcifications, and cerebellar and pontine atrophy.[14] In this case, the cortical changes depicted by MRI were interpreted as lissencephaly, polymicrogyria, and pachygyria. Polymicrogyria was suspected in the frontal lobes visualized by MRI (not shown), but the microscopic examination did not confirm it. Instead, focal glioneuronal outbursting into the subarachnoid space associated with coalescent calcifications at the cortical–white matter border, with heterotopias below them, could be responsible for the polymicrogyric cortical feature seen on MRI. The computed axial tomography, used to diagnose microcephalic infants after intrauterine Zika virus infection, showed bandlike calcifications and localized them more precisely, which corresponded to our findings.[23,24] Importantly, our neuropathologic evaluation demonstrated that the Zika virus–infected fetal brain shares most of the neuroimaging changes seen in other intrauterine TORCH infections and even in pseudo-TORCH phenotypes.[6,7,8,25,26] It is difficult to make a comparison with the neuropathology of such cases because relatively few autopsies with brain examinations have been performed,[27] not only in cases of Zika virus–associated microcephaly but also in other intrauterine fetal brain infections.[28,29] Some changes, especially those of a malformed cortex, have frequently been described as *polymicrogyria* on MRI, which should be interpreted with caution.[30] In addition to our case, an autopsy analysis of 8 other fetuses and infants with microcephaly caused by Zika virus has been reported, with concordance of the spectrum of overlapping gross and microscopic findings.[12,21,27,31] To our knowledge, however, glioneuronal outbursting into the subarachnoid space, which was observed in our case, has not been described in any other case of intrauterine brain infection. Additional detailed neuropathologic examinations from autopsies of infected fetuses and infants would be valuable toward increasing our understanding of the cortical pathology caused by the Zika virus.

We thank Marija Zupančič, Daniel Velkavrh, Breda Nagode, BSc, and Miha Juvan for technical support and the patient for her permission to publish the case. The mother of the fetus has signed a written agreement to the publication of our findings.

References

1. Abuelo D. Microcephaly syndromes [review]. *Semin Pediatr Neurol*. 2007; 14(3):118–127.
2. Mochida GH. Genetics and biology of microcephaly and lissencephaly. *Semin Pediatr Neurol*. 2009;16(3):120–126.
3. Bale JF Jr. Fetal infections and brain development. *Clin Perinatol*. 2009; 36(3):639–653.

4. Panchaud A, Stojanov M, Ammordorffer A, Vouga M, Baud D. Emerging role of Zika virus in adverse fetal and neonatal outcomes. *Clin Microbial Rev*. 2016;29(3):659–694.

5. França CM, Mugayar LRF. Intrauterine infections: a literature review. *Spec Care Dentist*. 2004;24(5):250–253.

6. Popa RT, Fayard C, Blondiaux E, et al. Imaging pattern in fetal CNS infections. Poster C-2491 presented at: the European Society of Radiology Meeting; March 1–5, 2012; Vienna, Austria. http://posterng.netkey.at/esr/viewing/index.php?module=viewing_poster&pi=109086. Accessed August 26, 2016. doi: 10.1594/ecr2012/C-2491.

7. Briggs TA, Wolf NI, D'Arrigo S, et al. Band-like intracranial calcification with simplified gyration and polymicrogyria: a distinct "pseudo-TORCH" phenotype. *Am J Med Genet A*. 2008;146A(24):3173–3180.

8. Kulkarni AM, Baskar S, Kulkarni ML, et al. Fetal intracranial calcification: pseudo-TORCH phenotype and discussion of related phenotypes. *Am J Med Genet A*. 2010;152A(4): 930–937.

9. De Carvalho NS, De Carvalho BF, Fugaça CA, Dóris B, Biscaia ES. Zika virus infection during pregnancy and microcephaly occurrence: a review of the literature and Brazilian data. *Braz J Infect Dis*. 2016;20(3):282–289.

10. Malone RW, Homan J, Callahan MV, et al. Zika virus: medical countermeasure development challenges [published online ahead of print March 2, 2016]. *PLoS Negl Trop Dis*. 2016;10(3):e0004530. doi:10.1371/journal.pntd.0004530.

11. Mlakar J, Korva M, Tul N, et al. Zika virus associated with microcephaly. *N Engl J Med*. 2016;374(10):951–958.

12. Driggers RW, Ho CY, Korhonen EM, et al. Zika virus infection with prolonged maternal viremia and fetal brain abnormalities. *N Engl J Med*. 2016; 374(22):2142–2151.

13. Oliveira Melo AS, Malinger G, Ximenes R, Szejnfeld PO, Sampaio SA, Bispo de Filippis AM. Zika virus intrauterine infection causes fetal brain abnormality and microcephaly: tip of the iceberg? *Ultrasound Obstet Gynecol*. 2016;47(1):6–7.

14. de Fatima Vasco Aragao M, van der Linden V, Martens Brainer-Lima A, et al. Clinical features and neuroimaging (CT and MRI) findings in presumed Zika virus related congenital infection and microcephaly: retrospective case series study [published correction appears in *BMJ*. 2016;353:i1901]. *BMJ*. 2016;353: i1901. doi:101136/bmj.i3182.

15. Werner H, Fazecas T, Guedes B, et al. Intrauterine Zika virus infection and microcephaly: correlation of perinatal imaging and tree-dimensional virtual physical model. *Ultrasound Obstet Gynecol*. 2016;47(5):657–660.

16. Chitra TV, Panicker S. Maternal and fetal outcome of dengue fever in pregnancy. *J Vector Borne Dis*. 2011;48(4):210–213.

17. Basurko C, Carles G, Youssef M, Guindi WEL. Maternal and fetal consequences of dengue fever during pregnancy. *Eur J Obstet Gynecol Reprod Biol*. 2009;147(1):29–32.

18. Alpert SG, Fergeson J, Noel LP. Intrauterine West Nile virus: ocular and systemic findings. *Am J Ophthalmol*. 2003;136(4):733–735.

19. European Centre for Disease Prevention and Control. Rapid risk assessment: Zika virus epidemic in the Americas: potential association with microcephaly and Guillain-Barré syndrome. Stockholm, Sweden: ECDC. http://ecdc.europa.eu/en/publications/_layouts/forms/Publication_DispForm.aspx?List=4f55ad51-4aed-4d32-b960-af70113dbb90&ID=1413. Published December 10, 2015. Accessed August 26, 2016.

20. Schuler-Faccini L, Ribeiro EM, Feitosa IM, et al; Brazilian Medical Genetics Society—Zika Embryopathy Task Force. Possible association between Zika virus infection and microcephaly—Brazil, 2015. *MMWR Morb Mortal Wkly Rep*. 2016;65(3):59–62.

21. Martines RB, Bhatnagar J, Keating MK, et al. Evidence of Zika virus infection in brain and placental tissue from two congenitally infected newborns and two fetal losses—Brazil, 2015. *MMWR Morb Mortal Wkly Rep*. 2016;65(6): 159–160. http://www.cdc.gov/mmwr/volumes/65/wr/pdfs/mm6506e1er.pdf. Published February 19, 2016. Accessed July 28, 2016.

22. Brasil P, Pereira J Jr, Raja Gabaglia C, Darmasceno L, Wakimato M, Ribeiro Nogueira RM. Zika virus infection in pregnant women in Rio de Janeiro—preliminary report. *N Engl J Med*. 2006;374(10):951–958.

23. Cavalheiro S, Lopez A, Serra S, et al. Microcephaly and Zika virus: neonatal neuroradiological aspects. *Childs Nerv Syst*. 2016;32(6):1057–1060.

24. Moron AF, Cavalheiro S, Milani HJF, et al. Microcephaly associated with Zika virus infection: neonatal neuroradiological aspects. *BJOG*. 2016;123(8): 1265–1269. doi:10.1111/1471-0528.14072.

25. Schwartz DA. The origins and emergence of Zika virus, the newest TORCH infection: what's old is new again [published online ahead of print October 20, 2016]. *Arch Pathol Lab Med*. doi:10.5858/arpa.2016-0429-ED.

26. Alvarado MG, Schwartz DA. Zika virus in pregnancy, microcephaly and maternal and fetal health: What we think, what we know, and what we think we know [published online ahead of print September 16, 2016]. *Arch Pathol Lab Med*. doi:10.5858/arpa.2016-0382-RA.

27. Schwartz DA. Autopsy and postmortem studies are concordant: pathology of Zika virus infection in neonates and stillborn fetuses with microcephaly following transplacental transmission [published online ahead of print August 24, 2016]. *Arch Pathol Lab Med*. doi:10.5858/arpa.2016-0343-OA.

28. Teissier N, Fallet-Bianco C, Delezoide AL, et al. Cytomegalovirus-induced brain malformations in fetuses. *J Neuropathol Exp Neurol*. 2014;73(2):143–158.

29. Courtier J, Schauer GM, Parer JT, Regenstein AC, Callen PW, and Glenn OA. Polymicrogyria in a fetus with human parvovirus B19 infection: a case with radiologic-pathologic correlation. *Ultrasound Obstet Gynecol*. 2012;40(5):604–606.

30. Barkovich AJ. Current concepts of polymicrogyria. *Neuroradiology*. 2010; 52(6):479–487.

31. Martines RB, Bhatnagar J, de Oliveia Ramos AM, et al. Pathology of congenital Zika syndrome in Brazil: a case series [published online ahead of print June 29, 2016]. *Lancet*. 2016;388(10047):898–904. doi:10.1016/S0140-6736(16)30883-2.